DATABASE OF POTENTIAL SOURCES FOR
EARTHQUAKES LARGER THAN MAGNITUDE 6
IN NORTHERN CALIFORNIA
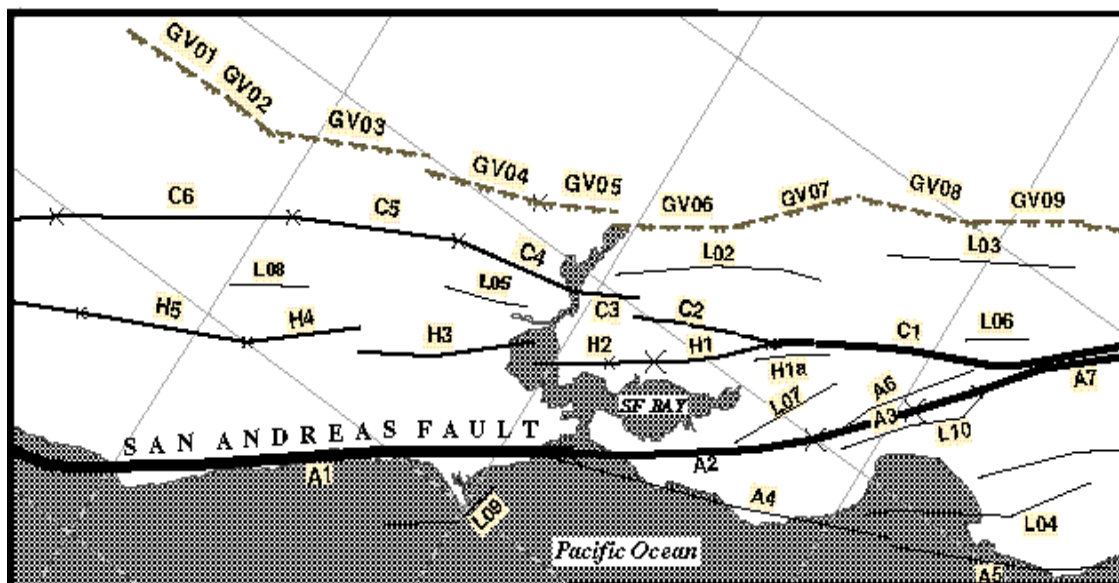
By The
Working Group on
Northern California Earthquake Potential

Open-File Report 96-705

1996

Working Group on Northern California Earthquake Potential

William Bakun	U.S. Geological Survey
Edward Bortugno	California Office of Emergency Services
William Bryant	California Division of Mines & Geology
Gary Carver	Humboldt State University
Kevin Coppersmith	Geomatrix
N. T. Hall	Geomatrix
James Hengesh	Dames & Moore
Angela Jayko	U.S. Geological Survey
Keith Kelson	William Lettis Associates
Kenneth Lajoie	U.S. Geological Survey
William R. Lettis	William Lettis Associates
James Lienkaemper*	U.S. Geological Survey
Michael Lisowski	Hawaiian Volcano Observatory
Patricia McCrory	U.S. Geological Survey
Mark Murray	Stanford University
David Oppenheimer	U.S. Geological Survey
William D. Page	Pacific Gas & Electric Co.
Mark Petersen	California Division of Mines & Geology
Carol S. Prentice	U.S. Geological Survey
William Prescott	U.S. Geological Survey
Thomas Sawyer	William Lettis Associates
David P. Schwartz*	U.S. Geological Survey
Jeff Unruh	William Lettis Associates
Dave Wagner	California Division of Mines & Geology
John Wakabayashi	Consultant
Gerald Weber	Weber, Hayes & Associates
Patrick L. Williams	U.C. Berkeley Seismographic Station
Ivan Wong	Woodward-Clyde Inc.
Robert H. Wright	Harlan Tait Associates

*Co-chair

CONTENTS

Abstract

The Northern California Earthquake Potential (NCEP) working group, composed of many contributors and reviewers in industry, academia and government, has pooled its collective expertise and knowledge of regional tectonics to identify potential sources of large earthquakes in northern California. We have created a map and database of active faults, both surficial and buried, that forms the basis for the northern California portion of the national map of probabilistic seismic hazard. The database contains 62 potential sources, including fault segments and areally distributed zones. The working group has integrated constraints from broadly-based plate tectonic and VLBI models with local geologic slip rates, geodetic strain rate, and microseismicity. Our earthquake source database derives from a scientific consensus that accounts for conflict in the diverse data. Our preliminary product, as described in this report brings to light many gaps in the data, including a need for better information on the proportion of deformation in fault systems that is aseismic.

Introduction

The working group began in late 1994, initiated by the regional program coordinator of the National Earthquake Hazards Reduction Program of USGS for the Northern California region, to assist in the preparation of National Seismic Hazard Maps [*Frankel and others*, 1996]. To meet the requirements for national maps of probabilistic seismic hazard, we set out to develop a map and database of potential sources of magnitude ≥6 earthquakes for the San Andreas fault system and northeastern California faults, using all available geologic and geophysical data north of 36° N and west of 120° W. *McCrory* [1996] has reported on the database for the Cascadian subduction zone separately. In later stages of the review process, we merged these USGS databases with a similar one prepared by the California Division of Mines and Geology (CDMG) [*Petersen and others*, 1996a,b]. It is this jointly developed CDMG-USGS database that was used to create both the USGS national and the CDMG state hazard maps. In turn these hazard maps form the basis for the design-ground-motion maps of the 1997 edition of the National Hazard Reduction Program Recommended Provisions for Seismic Regulations for New Buildings.

To assure public acceptance of resulting hazard maps and building codes, a scientific consensus was required on key parameters of potential earthquake sources such as magnitude and recurrence. The working group includes geologists and geophysicists from government, academia and industry who have worked with USGS toward a consensus fault model, which is a reasonable simplification of abundant, diverse scientific data. The model weights historical and paleoseismologic data heavily when available, otherwise accepted empirical scaling relationships are used. Regional strain data and plate tectonic models agree well with geologically measured slip rates on major faults, so regional hazard estimates are likewise well-constrained.

In the sections that follow, we will first discuss how in general we determined the key parameters in the database, then we present our consensus results for each major fault zone or region, and finally we will discuss the internal consistency of our results in comparison to broader regional models such as Nuvel-1A, VLBI observations, and historical rates of seismicity.

Methodology

Because the historical record of earthquakes in this region is so brief and many faults have neither ruptured in this historic period nor are paleoseismic data available, for most fault zones we had to rely on set of empirical relationships between fundamental earthquake parameters which are described below. Throughout the text we will refer to a so-called *standard methodology* which presupposes a characteristic earthquake model for a given fault or segment of a fault [*Schwartz and Coppersmith*, 1984] and applies the procedures and assumptions as described below.

Fault segmentation or determination of source length (l)

The length of a potential earthquake source is an important parameter for estimating the potential size of an earthquake. Historical data on actual rupture length are most preferred, followed by paleoseismic evidence. Most faults have neither, so current practice relies strongly on a combination of analogy to similar faults or by judgment based on available data of diverse character: *e.g.,* major bends or discontinuities in surface trace or microseismicity alignment are commonly chosen as segment boundaries. In northeastern California proximity to active volcanic centers offers distinct constraints on segment lengths. Tentative segmentation models adopted here are only intended for hazard modeling purposes. The endpoints should be treated as approximate in the seismic hazard analysis. Future paleoseismologic investigation is still required in all cases to test our currently preferred model. For fault location we primarily used a digital version of *Jennings* [1992] state fault map, but amended this map where greater accuracy was required (*e.g.,* San Andreas, Hayward, Northern Calaveras, Concord and Green Valley faults) or where mapping was incomplete for our purposes (*e.g.,* blind thrust faults of the Great Valley).

Fault down-dip width (w)

Generally we assumed 12 km as a typical value of rupture depth in Northern California used to calculate down-dip width. David Oppenheimer and Ivan Wong reviewed the database and suggested revisions based on USGS Calnet catalog and special investigations. Dip values were taken from a variety of sources, both geologic and seismologic.

Magnitude (M_w)

When reliable historical values of magnitude were available, then they were used. Otherwise, we mostly relied on the empirical relation of moment magnitude to rupture area (**a**=**lw**) of *Wells and Coppersmith* [1994](W&C94):

$$\mathbf{M}_w = 4.07 + 0.98 \log \mathbf{a} \ (\text{km}^2)$$

The equation using area was used in preference to the length equation because it is statistically more robust according to Wells and Coppersmith. Another important reason to avoid the length equation is that a great many of the events used to develop the equation have greater rupture width than applies to northern California, thus these wider ruptures have larger seismic moment than events of equal rupture length in California. Figure 1 and Table 1 illustrate that historic earthquakes in northern California generally agree better with the W&C94 area relation than with their length relation. Exceptions will be discussed by individual fault zone.

Average coseismic slip (d)

We used reliable historical or paleoseismological values of coseismic slip where available, otherwise, we derived slip from magnitude generally using the relation of moment magnitude to moment of *Hanks and Kanamori* [1979]:

$$\mathbf{M_w} = (2/3)\log\mathbf{M_o} \text{ (dyne-cm)} - 10.7$$

Using the definition of seismic moment ($\mathbf{M_o}$) and rigidity ($\mu = 3*10^{11}$ dyne/cm^2) gives average coseismic slip:

$$\mathbf{d} = \mathbf{M_o}/(\mu\mathbf{a})$$

Long-term slip rate (r)

Only minimum values of geologic or long-term slip rates are available for some larger faults in the region, because they may not represent the entire breadth of the fault zone. Local and regional geodetic strain rates and regional plate tectonic models have been used to check and constrain geologic rates where needed. Slip rate is often the most important indicator of a fault for earthquake potential, because it is strongly related to recurrence time. For this reason the database gives a range of slip rate that may be valid as an important measure of reliability of the model.

Recurrence time (t)

When reliable historical and paleoseismic values of average recurrence time (**t**) for events were available, then they were used. Otherwise, we continue to make use of the empirical relationships above and the following equation:

$$\mathbf{t} = \mathbf{d}/\mathbf{r}$$

where **d** is average coseismic slip (as above) and **r** is slip rate (as above). When considerable aseismic slip or creep occurs on a particular fault, then both the values of average slip and long-term slip rate must reflect the fault behavior in the seismogenic zone at depth. Coseismic surface slip can be much smaller than deep coseismic slip on creeping faults [*Oppenheimer and others,* 1990; *Lienkaemper and others,* 1991; *Lienkaemper and Prescott*, 1989]. Recurrence is a critical parameter for the probabilistic aspect of the hazard map. Sources with recurrence times of ≥20,000 yr will have little impact on the final maps.

Fault Zones

San Andreas and San Gregorio fault subsystem

The great 1906 earthquake, M_w~7.9, the predominant historic seismic event of the San Andreas fault system (SAFS) in northern California, ruptured all currently locked segments of the fault (**A1** in Figure 2a), from near the Mendocino triple junction (MTJ) to San Juan Bautista (SJB), where the dominantly creeping segment (**A7**) begins southward to Parkfield [*Thatcher and others,* 1997]. The 1906 rupture (**A1**) overlaps the ("independent") subsegments **A2** and **A3**, and southward to the point labeled "END 1906". Current research into prehistoric events along the northern San Andreas fault indicates that a similar great event probably occurred most recently in the 17th century [*Schwartz and*

others, 1997], thus it is reasonable that our model of the SAFS be structured around slip accumulation and release in great earthquake cycles that are about two centuries long or somewhat longer (*e.g.,* we use 210 yr ≈ 5.1 m/0.024 m/yr, the average 1906 slip north of the Golden Gate divided by the long-term slip rate, see below). The 1906 rupture on the San Andreas fault had distinct variations in coseismic slip along strike (Figure 3) based on the improved analyses by *Thatcher and others* [1997] of the historic triangulation data. The 330-km north coast subsegment of the fault, north of the Golden Gate, averaged 5.1 m of slip excluding the extremely high slip modeled near the MTJ. In contrast, south of the Golden Gate, 1906 slip averaged 3.4 m and 2.5 m for segments of the San Francisco Peninsula and Santa Cruz Mountains respectively. This reduction in 1906 slip at the Golden Gate has important implications for segmentation and for developing a recurrence model that is consistent with regional plate boundary conditions as well as local observations of events and slip rates.

The abrupt drop in 1906 slip at the Golden Gate may be explained in part by a ~2-km right stepover here in the San Andreas fault [*Cooper,* 1973], because such extensional zones tend to inhibit propagation of a rupture. Additionally, the San Gregorio fault (**A4**) branches away from the San Andreas near the Golden Gate, offshore of the City of San Francisco. The San Andreas slip rate of ~ 22-24 mm/yr north of the Golden Gate drops to ~ 17 mm/yr to the south. We deduce that most or all of the San Andreas decrease of ~5 mm/yr to the south occurs as slip lost to the San Gregorio fault. Thus, the San Gregorio fault is effectively a branch of the San Andreas fault with regard to the accumulation of slip over multiple great earthquake cycles. A cartoon (Figure 4) shows a reasonable model of slip accumulation that satisfies our current knowledge of historical and prehistoric earthquakes on the two fault zones considered jointly. Detailed discussions of individual fault segments follow. The important idea that emerges is that of *effective recurrence time* (**t_e**) between earthquakes on a given fault segment, that is the time between earthquakes on that segment considered independently of great or multisegment (M~7.9) ruptures. Especially important is the consideration of how slip on the San Gregorio fault (**A4**) relates to the recurrence times of events on the Peninsula segment (**A2**) of the San Andreas fault because jointly they must keep pace with ~5 m of slip per event on the San Andreas fault north of the Golden Gate. Usually, recurrence time only accounts for how often fault-rupture occurs at a particular point along the fault, but ignores whether the magnitude of the earthquake is a 7 or an 8. Probabilistic seismic hazard analysis must consider the *effective time*(**t_e**) between events of a *particular size* on a particular segment.

Peninsula segment (A2)

The San Francisco Peninsula segment of the San Andreas fault has been previously considered for purposes of earthquake forecasting to extend from north of the prominent bend in the fault through the Santa Cruz Mountains to south of the Golden Gate [*Working Group on California Earthquake Probabilities, (WGCEP)* 1988; 1990]. The occurrence of a major earthquake in this vicinity in 1838 [*Louderback,* 1947] and the apparent deficiency of slip in 1906 suggested that M7 events were likely on the Peninsula between great earthquakes. Historical evidence of the 1838 earthquake does not strictly constrain the source to be the San Andreas fault, so the segmentation model is necessarily speculative. In approaching segmentation, the *WGCEP* [1990] did not have the advantage of *Thatcher and others'* [1997] analysis of 1906 slip variation that makes the Golden Gate a simple choice for a northern segment boundary. Arguments about the southern segment boundary become complicated by details of fault geometry, but for our purposes the

northern end of the 1989 Loma Prieta rupture seemed a reasonable and cautious choice of segment boundary.

Hall and others [1995] measured slip of ~1.6 m on a buried offset stream channel at the Filoli trenching site that they associated with the penultimate earthquake on the Peninsula segment (event preceding 1906). Although the date of this penultimate event was not constrained stratigraphically, the 1838 earthquake is a permissible interpretation and seems reasonable. Because 1906 slip was ~2.5 m near Filoli, their data support the hypothesis of two distinct characteristic events for this segment (*e.g.,* **A1**-type of M_w 7.9 and **A2-**type of M_w 7.1 as described in the database; Table A-1 in Appendix A). For a M_w 7.1, independent Peninsula segment rupture (in 1838?), using the area formula of *Wells and Coppersmith* [1994] and other relationships described in our standard methodology, we expect average slip of 1.5 m on an 88-km-long rupture.

Slip rate for this segment of the San Andreas fault is still not constrained as well as for some other major faults. However, the Filoli site has also yielded a minimum slip rate of 14.8 ± 2.7 mm/yr over a time of 2.1 ka [*Hall and others,* 1995]. As is common with trenching data, the offset features used to measure slip rates do not span the entire active fault zone, so that the full slip rate could be greater. A higher estimate of 19 mm/yr derives from dividing the dextral slip of ~1.6 m accompanying the 1989 Loma Prieta earthquake [*Lisowski and others,* 1990] by the 83 yr since the 1906 earthquake which is assumed to have fully relieved the dextral strain, but as we discuss below this incorrectly assumes that 1989 is a characteristic San Andreas fault event. Another approach is to take the well-determined value of slip rate for the central San Andreas fault of ~34 mm/yr [*Sieh and Jahns,* 1984] and deduct from it the ~17 mm/yr of strain that is conveyed to the southern Calaveras fault system [*Savage and others*, 1979], leaving ~17 mm/yr for the San Andreas fault northward of San Juan Bautista. We have adopted 17 ± 3 mm/yr for the segment **A2** because we find it consistent within expressed limits of error considering a broad range of reasonable arguments from local data, regional kinematics and strain, and also plate boundary and VLBI constraints as will be discussed later.

Recurrence time is not yet established by prehistoric evidence on the Peninsula, thus we had to rely on a hypothetical strain accumulation model (Figure 4). In this model, the Peninsula keeps pace with the SAF slip accumulation on the north coast by having an equal number of San Gregorio events each of ~2 m of slip and independent Peninsula San Andreas events of ~1.6 m at an effective recurrence time (t_e) for **A2** type events equalling two recurrence times of great SAF earthquakes for each, hence ~ 400 yr.

Santa Cruz Mountains segment (A3)

We have adopted the extent of the M_w 6.9 Loma Prieta earthquake source region of 1989 to define the Santa Cruz Mountains segment, however much about this event does not fit the ideal of a characteristic earthquake, especially the sizable dip-slip component and the mismatch of the 6-17 km deep, dipping 1989 rupture surface determined from aftershock locations with a near-vertical orientation generally expected for ruptures associated with the main trace of the San Andreas fault that ruptured in 1906. It remains uncertain whether there really is a characteristic earthquake for this segment that is independent of great San Andreas fault earthquakes. The location of the large 1865 earthquake may not have been on the San Andreas fault [*Tuttle and Sykes,* 1993]. *Schwartz and others* [1997] find no evidence for any earthquake except the 1906 rupture on the main trace of the San Andreas fault in this segment since the 17th century. Nevertheless, a high long-term slip rate and low slip here in 1906 require that earthquakes occur frequently near here, either on the San Andreas fault or other nearby structures. Thus

we assume an idealized event with the same dextral slip and rupture extent as the 1989 event but having an effective recurrence time (t_e) of 400 yr. Such events on a Santa Cruz Mountain segment could, taken in combination with San Gregorio fault events and great (*e.g.,* 1906) events, keep this segment in synchrony with the cycles of ~5–m of strain accumulation and release that we assume for the San Andreas fault north of the Golden Gate. Slip rate of 14 mm/yr reflects a loss of ~3 mm/yr dextral slip from the ~17 mm/yr assumed available on the Peninsula segment of SAF to the Sargent fault and a complex of other known and unknown structures in the Santa Cruz Mountains.

San Gregorio fault (A4, A5)

The north end of the San Gregorio fault segment (**A4**) is generally accepted as a branching connection to the San Andreas near the Golden Gate. Because most of this fault zone is offshore, the map details of the active trace are obscure but allow that the trace may be generally straight for the 129 km from the Golden Gate branch point south to Monterey Bay where a 2-3 km right stepover exists. Although slip rate data are not available for the San Gregorio fault in the Sur region (**A5**), the southernmost San Gregorio fault system or Hosgri fault zone near San Simeon are believed to have a lower rate than segment **A4**. Because the Monterey Bay-Tularcitos fault zone (**L04**) appears to branch off near this right stepover, we assume that it is kinematically reasonable that the southward decrease in slip on the San Gregorio fault zone may occur at least partially near this branch point and that farther southward some of this slip may next transfer to the Rinconada fault (**L01**).

Quaternary and Holocene slip rates along the San Gregorio fault have been difficult to constrain narrowly, partly because much is offshore and because much of the fault has highly complex geometry. For the northern segment (**A4**) we assume ~5 mm/yr because preliminary work at Seal Cove on two different-aged markers (see Table A-1 for references) seems to force this result. Other sites permit a broader range of slip rate, so we must regard this rate as preliminary. The southern segment (**A5**) has no slip rate data, but to the south data support a rate of ~3 mm/yr (see Table A-1).

Estimates of average recurrence time of earthquakes, loosely constrained by fault offset on archaeological layers at the Seal Cove sites, range from 350 to 680 yr for the last two events (G. D. Simpson and others, 1995, writ. com.) Horizontal offset of these layers suggest that events have coseismic slips of >2 m. We use a hypothetical 400 yr effective recurrence time estimated from our hypothetical San Andreas-San Gregorio slip accumulation cartoon (Figure 4). Our standard methodology yields recurrence of 330 yr and slip of 1.7 m. Our hypothetical recurrence time is a moderate value and errs on the side of caution, but we recognize that considerably longer recurrence times also satisfy existing data.

For the Sur region segment (**A5**) we determined all segment parameters by our standard methodology and by comparison to the adjacent segments: the estimated 400-yr recurrence is coincidentally in phase with the segment to the north (**A4**) and we use the ~3 mm/yr slip rate of the Hosgri segment which lies to the south of a major structural discontinuity (Table A-1).

Related faults

The Sargent fault (**A6**) has ~3 mm/yr dextral creep rates measured (see Table A-1) in its central part where traces are distinctly Holocene and dominantly right-lateral in their geomorphic appearance [*Bryant and others,* 1981]. Evidence for recency is more obscure in the steep and heavily vegetated terrain to the north where a larger dip-slip component is required to accommodate volume problems at the junction with the San Andreas fault.

Our chosen source model is for a hypothetical event using a maximum length and applying our standard methodology. The "Sargent" event is intended in part as an approximate representation of additional hazard that probably exists in the region where the San Andreas fault bends and splays in the Santa Cruz Mountains. This additional hazard is not strictly confined to the main trace of the San Andreas. Some minor faults such as the Zayante (**L10**) and Shannon-Monte Vista (**L07**) also address this issue, but are of nearly negligible impact compared to the Sargent and related faults. Preliminary values of slip rate (0.6 mm/yr) and recurrence time (1200 yr) have been suggested by *Nolan and others* [1995] from a paleoseismic investigation on the southernmost Sargent fault, however both values derive from speculative interpretations using vertical separations and a broad range of low-angle rakes on slickensides to infer slip vectors. We use the larger slip rate inferred from measured surface creep as a minimum and the resulting short recurrence time from our standard methodology because they are not excluded by the preliminary paleoseismic work and are a more cautious assumption for hazard analysis.

Preliminary versions of our database assumed a short segment of the San Andreas between the Santa Cruz Mountains and the southern end of the 1906 rupture at San Juan Bautista. A M~6 earthquake occurred in this region in 1890, but was not indisputably located on the San Andreas. Such an event has little impact on the hazard analysis because it is in the range that will be reasonably modeled as background seismicity. Hence this speculative segment was deleted as a source of independent large earthquakes. In 1836 a sizable earthquake, M~6.5 ± 0.5, apparently happened on some fault in the region around San Juan Bautista; this event had been mistakenly associated with the Hayward fault [*Toppozada and Borchardt*, 1997]. The San Andreas south of this segment is treated as fully creeping (**A7**) and events less than about M~6 will be adequately modeled as background seismicity.

Hayward fault subsystem

1868 earthquake

The Hayward fault (**H1** and **H2** in Figure 2) had at least one major historical earthquake in 1868. *Lawson* [1908] stated that the surface rupture in 1868 extended at least from Agua Caliente Creek (AC in Figure 5) northerly to San Leandro (SL), and less certainly to Mills College (MC). Recent trenching investigation [*Lienkaemper and others,* 1995] and analysis of 19th-century triangulation data [*Yu and Segall,* 1996] suggest that sizable slip occurred as far north as northern Oakland (MT, Montclair trench; BT, BART tunnel). We assume that the location of the southern termination of the 1868 subsurface rupture, at the base of the seismically active crust, coincides with the point where most slip is transferred from the Calaveras to Hayward fault. High creep rate (9-10 mm/yr) occurs on the Calaveras fault north of Halls Valley (HV). North of Calaveras Reservoir (CR) creep on the Calaveras fault is 3-6 mm/yr. We deduce that the high creep rates (9 mm/yr) that occur on the Hayward fault from Agua Caliente Creek (AC) northward [*Lienkaemper and others,* 1991] indicate that the main subsurface connection of creep between the Calaveras and Hayward faults lies north of the line between Halls Valley and Agua Caliente Creek. Because the microearthquakes (Figure 5) that connect the southern Hayward fault to the Calaveras fault have dominantly strike-slip focal mechanisms, the connection of deep slip probably occurs along a path associated with these small earthquakes [*Ellsworth and others,* 1982; *Wong and Hemphill-Haley,* 1993].

Probably the most accurate measurement of the size of the 1868 earthquake comes from modeling 19th-century triangulation data by *Yu and Segall* [1996]. Their best-fitting

model suggests 1.9 ± 0.4 m slip and M_w 7.0. Trenching evidence [*Lienkaemper and others*, 1995] at Montclair (MT) in north Oakland suggests that much larger slip occurred there in the previous earthquake (pre-1776; *Toppozada and Borchardt*, 1996) than in 1868, however this apparent conflict with the triangulation results could be easily explained if the large pre-1776 slip here was mainly shallow and the large 1868 slip was deeper (*i.e.*, underlies the pre-1776 patch in the presumed overlap) as we show in a cartoon, Figure 6. The patch areas shown in Figure 6 yield M_w 7.0 for 1868 and 6.9 for the pre-1776 northern event assuming 1.9 m average slip over 12-km-deep ruptures for both events. Using the methodology of *Savage and Lisowski* [1993] and the regional slip rates of the NCEP database, the effect of strain reduction by creep in the upper 5 km of the fault zone (~7%) is not likely to be important to these calculations (*i.e.*, fault zone is 93% locked and M_w is reduced only 0.02 by the surficial creep). These assumptions lead to a 210-yr recurrence time for major earthquakes on both segments which is the same as the best estimate of recurrence of *Williams* [1993] for the southern Hayward Fault based on trenching data at Tule Pond [TP] in Fremont. We do not know how the magnitude and length of the 1868 event compares to earlier events, because the paleoseismic record is not adequate to compare the size of events. If the entire 86-km length ruptured with 1.9 m slip it would be M_w 7.1. Adding the southeastern extension of the fault (**H1a**) to produce a 112-km rupture would still only produce a M_w 7.2 because its slip rate is much lower, ~3 ± 2 mm/yr.

The actual segmentation and recurrence history of the Hayward fault remains highly uncertain. Previously, it was widely assumed that the last major event associated with rupture on the northernmost Hayward fault occurred in 1836, but this association apparently was mistaken [*Toppozada and Borchardt*, 1997] . Because we do not know which segmentation models are likely to be correct, our database divides the entire fault into two equal parts of 43-km length. The northern extent of the fault under San Pablo Bay was truncated to reflect the right-stepover and transfer of slip to the Rodgers Creek fault, thus leaving no overlap and duplication of seismic moment release. Coseismic slip of 1.9 m and 12 km depth of rupture [*Oppenheimer and others*, 1993] produces M_w 6.9 events for each hypothetical segment. We cannot currently conclude that the two segment model is more likely than a scenario involving the entire length, so we rank them equally likely. *Petersen and others* [1996a, b] chose to retain the 1.5 m slip and 167 yr recurrence time adopted by *WGCEP* [1990] for two Hayward fault segments, that also yields M_w 6.9 and an identical rate of moment release, but they felt it was a more cautious assumption given the great uncertainties in recurrence time.

Rodgers Creek fault

The Rodgers Creek fault (**H3**; Figure 2a and 8) is believed to be entirely locked (*i.e.*, no recognized creep, <2 mm/yr; *Galehouse*, 1995; USGS trilateration data, 1978-88) and has not had a major historical earthquake. Segmentation is fairly straightforward because the fault terminates both northward at **H4** and southward at **H2** in distinct right stepovers of a few kilometers width. In consultation with CDMG we chose to simplify segmentation by eliminating the overlaps of **H3** with **H4** and **H2**, so that seismic moment would not be duplicated in the hazard analysis. Actual ruptures would be expected to taper into the stepover overlap region in some complex way. We have adopted the 230 ± 130 yr paleoseismic recurrence time based on 3 events and characteristic coseismic slip of ~2 m from *Schwartz and others* [1993]. This slip yields M_w of 7.0. Slip rate of 8.4 ± 2 mm/yr by *Schwartz and others* [1993] suggests that the 9 mm/yr used on the Hayward fault be adopted for the Hayward fault subsystem north of San Pablo Bay as well.

Calaveras fault subsystem

Southern Calaveras fault (C1)

At its south end, the southern Calaveras fault (**C1**) diverges from the fully creeping central San Andreas fault (**A7**) gaining nearly half of the central San Andreas' 34 mm/yr slip rate. The southern Calaveras branches into the Northern Calaveras and Hayward faults by the south end of Calaveras Reservoir (CR, Figure 5). The southernmost Calaveras-Paicines fault zone, ~80-km long, that extends from San Benito to Coyote Reservoir has previously been assumed not to have large earthquakes because its creep rate is high (12-17 mm/yr) and matches its long-term or geologic slip rate within the limits of uncertainty [*Bakun and others,* 1986; *Harms and others,* 1987; *Perkins and Sims,* 1988; *Sims,* 1991]. South of Hollister the Calaveras is located only 3-5 km away from and parallel to the San Andreas fault, thus may not be an independent source of large earthquakes. We suggest that the 1984 Morgan Hill earthquake, M_w 6.2, is a reasonable maximum magnitude event to occur in these segments, so rather than apply a detailed segmentation model we chose to assume that such an event has an equal likelihood of occurring anywhere along the entire southern Calaveras fault.

Northern Calaveras fault (C2)

The Northern Calaveras fault (**C2**) extends from Calaveras Reservoir (CR, Figure 5) to its north end, a right stepover to the Concord fault (**C3**). Based on simple geometric interpretation of the surface trace, this fault can be divided in three segments of roughly similar lengths [*Simpson and others,* 1993]. Thus, we have considered the reasonableness and practical impact of assuming that shorter single segment ruptures occur in addition to ruptures of the entire fault (**C2**).

San Ramon segment (C2c)

The San Ramon segment, **C2c**, has had at least one sizable earthquake historically in 1861 of roughly M6 (±0.5) and an apparently-associated ground rupture of about 13 km length from near Elworthy Ranch (ER, Figure 5) [*Rogers and Halliday,* 1993] to near Dublin Canyon (DC, Figure 5). Northward from Elworthy Ranch the fault has a less distinct geomorphic expression and trenching near Alamo (CA, Figure 5) [*Simpson and Lettis,* 1994] reveals no distinct evidence of Holocene slip on the main trace in well-stratified deposits of late Pleistocene to Holocene age. The northern end of the fault is a right step over of a few kilometers to the Concord fault (**C3**). Figure 5 shows recent microearthquakes that mark possible subsurface connections between the Northern Calaveras and Concord faults (M≥2, 1989-1995). Creep rate on this segment (Figure 5, triangle labeled SF-19) has increased significantly since the 1989 Loma Prieta earthquake, from near zero (0.4 ± 0.1 mm/yr, 1981-1989) to 2.7 ± 0.2 mm/yr (1989-1996) (J. S. Galehouse, writ. comm., 1996), similar to the ~3 mm/yr creep rates on the Concord fault and the Calaveras fault in Sunol.

Amador Valley segment (C2b)

The middle segment of the fault (**C2b**) may have ruptured in a M~6 earthquake in 1864, but the location of the event is poorly known and there was no report of surface rupture as there was for the 1861 earthquake. The length of this segment is controlled by two distinct right stepovers in the fault and thus could be expected to have its own earthquakes of M~6.

Sunol Valley subsegment

The southern subsegment of the Northern Calaveras, near Sunol Valley and Calaveras Reservoir (CR), appears to be the dominant source segment of much larger ground-rupturing earthquakes at Leyden Creek site (LC in Figure 5; *Kelson and others*, 1996). We assume that this Sunol Valley subsegment only ruptures along with the San Ramon (C2c) and Amador (C2b) segments, hence we do not have a separate entry in Table A-1 for an independent "C2a" source. Greater strength of this segment may be attributable to a 0.7-0.9 km left stepover located between Leyden and Welch Creeks that could act as a compressional asperity. A cartoon (Figure 7) illustrates how slip could accumulate at a rate of 6 ± 2 mm/yr over centuries as a combination of larger slip in major earthquakes that break the entire fault length of ~50 km and contributions of lesser events, such as the 1861 earthquake that break a smaller part of the fault. Our database includes both types of events with the effective recurrence of each weighted to reflect a combination of events that accumulates slip evenly along the fault and agrees with the current understanding of each segment's behavior from paleoseismologic and historical observations.

Recurrence time between major events could be as long as 550 ± 300 yr at Leyden Creek [*Kelson and others,* 1996], but our methodology yields 170 yr. *Bonilla and Lienkaemper* [1990] showed that even large historic surface ruptures sometimes cannot be recognized in trenches because of a variety of factors such as the contrastiness of geologic materials and effects of soil forming processes. To address this serious difference in recurrence estimates, a rounded intermediate value of 400 yr was adopted as a cautious estimate that reflects our considerable uncertainty in the fault's actual behavior. In the cartoon (Figure 7), two $M_w6.1$ events on both the San Ramon and Amador segments can occur for each $M_w7.0$ occurring on the entire Northern Calaveras fault. This model is only one of many possibilities that agree with the sparse and uncertain historical and paleoseismological data. An alternative approach for hazard analysis is to distribute the same seismic moment rate over a range of magnitudes and recurrence times [*Frankel and others,* 1996; *Petersen and others,* 1996a, b].

Concord-Green Valley faults

Although the overall zone is highly complex and includes some significant active secondary traces such as the Cordelia fault [*Harlan Tait Associates*, 1994], most of the working group felt that the Concord-Green Valley fault zone is likely to fail in one major event, but a few were concerned that a stepover capable of stopping ruptures might exist under Suisun Bay. A single event model (**C34**, Table A-1) involves a $M_w6.9$ every 180 yr, but the opposite alternative of independent Concord (**C3**) and Green Valley (**C4**) fault events would produce a $M_w6.5$ every 110 yr and a $M_w6.7$ every 150 yr respectively. In view of the absence of events on the two faults in the ~150+ yr historic record, the latter alternative seems somewhat suspect. The model given in our database is an average of these two opposing assumptions. Applying a Gutenberg-Richter distribution using a single segment model (**C34**) for maximum magnitude $M_w6.9$ every 180 yr achieves a similar result to our model [*Frankel and others,* 1996; *Petersen and others,* 1996a, b].

North Coast

The North Coast for the following discussion includes the Hayward and Calaveras fault subsystems that lie north of the metropolitan San Francisco Bay region (Figure 8: segments: **H4**, **H5**, **H6, H7, C5**, **C6**, **C7**, and **C8)**. In general, the Holocene fault traces in this region are rather poorly known, hence the continuity of microseismicity and locations of ongoing fault creep are especially important in locating and characterizing active traces.

No major historical earthquakes have been associated with specific North Coast fault segments, nor has paleoseismologic evidence yet clarified any characteristic behaviors of these faults.

Hayward fault subsystem, North Coast

The Maacama fault (**H4**, **H5**, **H6**) to the north has a sizable creep rate, ~7 mm/yr at Willits (on **H5**) and Ukiah (on **H6**)(see Table A-1; Figure 8). This large creep rate makes plausible our assumption that the 9 mm/yr long-term slip rate adopted for the Hayward and Rodgers Creek fault continues northward along the Maacama fault zone. As we discuss later, the observed geodetic strain rate and current global plate rate analysis support extending such a rate into the Garberville-Briceland segment (**H7**). The slip per event, ~2 m, that we adopted for the Hayward and Rodgers Creek, based on historic and paleoseismic data, is larger than the values expected for the lengths of these North Coast segments using our standard methodology. Hence, we continue to assume ~2 m slip per event for the North Coast segments: **H4**, **H5**, **H6,** and **H7**. Although the segment boundary from **H5** to **H6** is rather subtle, we felt that short segments were more comparable to the creeping Hayward fault (**H1** and **H2**) which appears to show some segmentation despite being an unusually straight and simple fault.

Calaveras fault subsystem, North Coast

The map location of the Holocene fault traces is especially uncertain for this fault subsystem in the North Coast region. The terrain is steep, landslides and vegetational cover are extensive, thus making difficult the usual procedures for delineating active faults, especially the geomorphic interpretation of aerial photography. Segmentation relied on weighted judgment based on the ages of various mapped Quaternary fault traces of *Jennings* [1992] and the density of microseismic activity.

Creep is recognized on all segments of the Calaveras fault subsystem in the San Francisco Bay area, so we expect it may continue into the North Coast but few data are available to test this assumption. On Figure 8 (lower), two velocity vectors straddle the Round Valley fault (**C7**), indicating creep of ~8 mm/yr, 1985-1989. Although the 5-6 yr duration of the survey is too brief to be highly exact, this demonstration of a sizable creep rate so near its north end may have important implications for the Calaveras fault subsystem as a whole. At least we may reasonably extend further northward our assumption of 6 mm/yr long-term slip rate with some greater assurance, but with some additional concern that it might be a low estimate.

Great Valley thrust faults

We use the 1983 Coalinga earthquake (**GV13**) as the principal example for segmentation of the Great Valley thrust fault system (Figure 9). *Stein and Ekstrom* [1992] modeled the leveling data from before and after the 1983 event. Their model is in accord with the focal mechanism of the mainshock, the 3-dimensional pattern of the aftershocks, and the interpretation of crustal and geologic structures of the region by Wentworth and Zoback [1989]. We used a simplified version of their favored thrust fault mechanism as a template for a thrust fault system that extends as far north as the Rumsey Hills (39° N) shown as segments **GV01** to **GV14**. Except for the northernmost two segments, a single rate of shortening 1.5 mm/yr is consistent with both the VLBI rate modeled for the Pacific plate-Sierran block boundary and local rates of uplift where such data were available [D.F.

Argus, written commun. 1995; *Wakabayashi and Smith* [1994]). *Unruh and Moores* [1992] and *Unruh and others* [1995a,b] show that the structural setting of the Sacramento Valley is also compatible with the same variety of thrust mechanism.

Segmentation follows the paradigm set by the Coalinga rupture. A stepover and a truncation of the principal antiformal structure adjoining the Great Valley synform axis distinctly limited the areal extent of the 1983 rupture [*Stein and Ekstrom*, 1992]. *Stein and Ekstrom* [1992] show by modeling years of postseismic deformation that aseismic slip probably continued downdip to 15 km, below the 7-10 km depth range attributed to the coseismic rupture. This postseismic creep is an important feature that tends to limit the amount of seismic moment available coseismically for such earthquakes, because we believe that slip between depths of 10-15 km occurs aseismically in this region. For segmentation, we mainly relied on major bends, stepovers and truncations of the principal antiformal structure immediately adjacent to the Great Valley synform. For comparison, in Figure 9 we show the generally similar segmentation results of *Wakabayashi and Smith* [1994] and of *Unruh and others* [1995b].

Minor faults in the San Andreas system

Frankel and others [1996] judged that faults with slip rates <0.1 mm/yr and lengths <15 km contribute negligibly to seismic hazard and that regional background seismicity rates reasonably accounted for hazards from such minor faults. Thus for the San Andreas system exclusive of the Great Valley thrusts, only ten low slip rate (≤2 mm/yr) faults remain in the final database as **L01** through **L10** and are listed in Table A1 in order of decreasing moment rate. Indeed, even many of these remaining faults probably have negligible impact on the regional seismic hazard, especially those that lie close to the major faults. The longest faults, such as Rinconada and Greenville, may well rupture in smaller segments, but in our final data table we indicate only a maximum rupture length, a maximum magnitude, and a proportionately long recurrence time. For all of these minor faults with maximum M_w>6.5 , the methodology of *Frankel and others* [1996] and *Petersen and others* [1996a, b] distributes half of the seismic moment rate into a Gutenberg-Richter function with a M_w 6.5 lower bound. Thus, an approximate likelihood of shorter segments and recurrence times is contained in the hazard analysis.

Northeastern California

We will begin our discussion of hazards in northeastern California with an overview of expected regional long-term rate of slip from global plate tectonics and compare that to geodetic, geological and seismological observations of the region and particular fault zones. Although abundant evidence of late Quaternary and Holocene faulting exists, several factors lead to considerable uncertainty in assigning the level of seismic activity expected from regional tectonics into discrete earthquake sources in this region. The most problematic factors are the great breadth and complexity of fault systems and the sparseness of Holocene deposits needed to judge recency of faulting and measure slip rates on particular faults. Hence, to account for seismic hazard we adopted four areal sources (Figure 2b, **NE09** - **NE12**) in consultation with workers in adjoining states to develop a consistent tectonic model. We also delineated eight linear zones (**NE01** - **NE08**) and discuss them in the context of the overall tectonic model.

Tectonic model for Northeastern California

Very Long Baseline Interferometry (VLBI) data show that considerable motion occurs between the generally rigid Sierra Nevada-Great Valley block and stable North

America plate (11±1 mm/yr toward N50°W evaluated at Quincy (Figure 2b; Figure 10), *Ward*, 1990; *Argus and Gordon*, 1991). Geodetic networks and VLBI are beginning to explain how crustal strain is distributed in the eastern, central and southern Great Basin [*Savage and others,* 1992, 1995; *Dixon,* 1995]. Some east-west normal faulting is mostly concentrated on the Wasatch fault at the eastern boundary of the Great Basin (Table 2, Figure 10, Figure 11). A zone of north-northwesterly trending dextral shear branches from the San Andreas fault system in southern California and north of the Mojave Desert follows the western margin of the Great Basin. A major branch of this zone of dextral-normal faulting broadly distributes strain throughout the Central Nevada Seismic Zone. VLBI evidence and geologic evidence demonstrate that dextral zones re-enter California as two branches (HL, Honey Lake fault and L-T TZ, Lassen-Tahoe tectonic zone in Figure 10). VLBI stations at Quincy and Hat Creek (HTC) have maintained a consistent velocity differential that averaged 3.6 mm/yr at ~N54°W for a decade (D. F. Argus, writ. commun., 1995). We suggest that this dextral shear reflects permanent aseismic deformation near the Lassen volcanic center that lies between the two sites and reflects strain release principally of the L-T TZ, but also may release strain from the branch associated with the Honey Lake fault. Geologic slip rate evidence on the Honey Lake fault suggests a minimum of 2 mm/yr dextral slip rate on that branch of the shear zone [*Wills and Borchardt,* 1993].

To develop a defensible regional tectonic model for northeastern California we chose to close a circuit of slip rate vectors from the Pacific plate near the San Francisco Bay region where data are plentiful, through the northeastern California area near Quincy, across the northern Great Basin where active faulting is sparse and closing to the North American plate east of the Wasatch fault (Figure 10). Using the Nuvel-1A [*DeMets and others, 1994*] and the most recent VLBI model for the Pacific plate-Sierra Nevada block motion is parsimonious because Nuvel-1A may represent a minimum estimate [*DeMets*, 1995] and the Pacific-Sierran block model is well-corroborated for the SF Bay region as we discuss below. We considered a narrow interpretation of plate tectonic modeling prudent because northeastern California is something like a concealed triple junction partly analogous to the Mendocino triple junction that lies to the west, thus a different tectonic regime may apply. The shear zones of northeastern California resemble the San Andreas fault system of coastal California in that they are largely dextral and driven by interaction with the Pacific Plate, whereas the high Cascade volcanic structures from Lassen Peak northward are more closely associated with Cascadian subduction than with the San Andreas fault system. Some tectonic models argue for a continuation of substantial dextral shear northward from California and Nevada into Oregon [*Wells*, 1990*; Pezzopane and Weldon,* 1993], but these models are not yet corroborated because adequate geologic slip rate data and the necessary geodetic coverage are lacking for the region. The vector difference of the total Nuvel-1A motion and current VLBI Sierran-Pacific model is 9.1 mm/yr directed N51°W. Subtracting known slip rate vectors in the Basin and Range outside of the northeastern California shear zone yields 6 mm/yr directed N33°W available within the dextral shear zone (Table 2). Because it probably has the largest slip rate of any normal fault in the Great Basin, we gave much consideration to the rate on the Wasatch fault. Geologic data permit at most ~1-2 mm/yr for the Wasatch fault sensu strictu, whereas geodetic data suggest at least ~3 mm/yr. Hence, we assume 2.5 ± 1 mm/yr is approximately correct but may either integrate slip rate of other northeastern Great Basin faults or neglect some regional strain associated with the entire intermountain seismic belt.

We partition ~2 mm/yr of the 6 mm/yr of available dextral shear onto the larger northeastern faults where geologic slip rates are generally minimum estimates (*e.g.,* **NE01**

16

and **NE02**) based on a single strand in a complex zone. Sources **NE03** and **NE04** are assumed to jointly continue the total slip rate of **NE02** northward as they are distinctly active faults compatible in their geomorphic expression and fragmental slip rate data with this assumption (W. A. Bryant, writ. comm., 1996). The areal source from western Nevada (**NE12**) is assigned 4 mm/yr. Northward from this source, areally distributed slip rate on **NE10 and NE09** is dropped to 2 mm/yr to reflect the contributions from specifically delineated fault zones (**NE02**, **NE03**, **NE04**) as discussed above. A small remainder, ~2 mm/yr of dextral shear directed N2°W, has been ignored in this analysis and could be presumed to be distributed in some highly uncertain way within the northern Great Basin between the Surprise Valley fault (**NE05**) and central Nevada.

Foothills fault zone (NE11)

We estimate that the slip rate of the Foothills fault system is well below the minimum of 0.1 mm/yr generally used as a filter in this study to eliminate low-activity faults that do not contribute to seismic hazard beyond the regional background level [*Frankel and others*, 1996]. However, because the fault zone has re-emerged as having continuing importance for engineering and major public policy reasons [*Schwartz and others,* 1996], we deemed it prudent to include this complex fault system as an areally distributed hazard (**NE11**).

Discussion

Plate vector and geodetic constraints

The consistency of the database or NCEP model can be tested in a variety of ways against broad regional constraints. We have already begun discussion of the most general plate tectonic constraint for the faults of northeastern California (Figures 10 and 12, Table 2). In Figure 11 we continue the vector summation started on the North American plate, and add the slip rates adopted for the northern Great Basin and the Sierra Nevada-Great Basin shear zone in northeastern California. We continue summation of slip rate vectors from our model along a path through the San Francisco Bay region. The net slip vector across the entire San Andreas System is nearly identical to the most recent VLBI results, but is slightly longer than the parsimonious Nuvel-1A model [*DeMets and others,* 1994; and *DeMets,* 1995]. The discrepancies between the VLBI, Nuvel-1A, and NCEP resultant vectors are so small (≤2 mm/yr or <5%) that they are not significant. We have ignored some minor additional compressional, fault-normal component on the San Gregorio fault [*Anderson and Menking,* 1994] and perhaps elsewhere in the Coast Range and continental borderland. *DeMets* [1995] suggested an additional dextral slip may occur outboard of the original plate model and that the Pacific-North American plate motion may have speeded up in the last 0.78 Ma. The regional crustal strain observations of *Lisowski and others* [1991] agree closely with the VLBI model shown in Figure 11, hence suggests that no significant offshore dextral strain occurs outside of the USGS trilateration network and that our NCEP model is complete for the San Andreas fault system. Thus our model and the VLBI model both support the possibility of a small recent increase in the plate motion compared to the 3.16 Ma average reflected in Nuvel-1A, but do not require it.

The plate vector test above demonstrates that the NCEP model is a good match to independent estimates of strain that can potentially accumulate in the system. A more rigorous extension of this test is to sum the total seismic moment rate included in the model for the entire San Andreas fault system (Tables 3 and 4). The result is 6.8×10^{18} Nmyr^{-1}. For a simple test of this result, we postulate a single straight fault that runs the

length of our modelled region as shown in Figure 12. This hypothetical structure extends 576 km from the north end of the 1966 Parkfield rupture (PKF) to the Mendocino triple junction (MTJ) and has the 12 km down-dip fault width typical of the northern Coast Range. Using the 39 mm/yr VLBI motion yields 8.1×10^{18} Nmyr^{-1}, but if one subtracts loss of seismic moment equivalent to the aseismic, 100-km-long creeping section of the San Andreas the result is 6.8×10^{18} Nmyr^{-1}, identical to the sum of moment rate for the NCEP model.

Comparison of NCEP model to historical seismic moment rate

Because the historical period (~1850-present) is short (145 yr) compared to the length of a major regional seismic cycle (recurrence time of 1906 San Andreas fault event ~210 or ~250 yr), we cannot assume that the flux of seismic moment is uniform enough to test our model. Nevertheless, we have summed the historic moments for the San Andreas fault system as shown in Figures 12 and 13. Despite the incomplete representation of the entire seismic cycle in the historical record the regional total for seismic moment rate has been 6.8×10^{18} Nmyr^{-1}. This match of the net historic seismic moment rate to both the sum of moment rate for the entire NCEP model, and to the sum derived from the simplified plate boundary test above is either a remarkable coincidence, or it may suggest some spatial and temporal partitioning of slip release in the historic period. Most of the Hayward and Calaveras fault subsystems have accounted for much less moment rate in the historic period than the San Andreas-San Gregorio subsystem. Possibly these lesser faults release strain earlier in the seismic cycle in preparation for the great San Andreas earthquakes. The historic record permits this possibility and future paleoseismological investigations could be initiated to test this idea. Great Valley thrust earthquakes also match the historic seismicity rates well, perhaps because they are relatively smaller and regionally-speaking are more frequent than events on the larger faults. On the northeastern faults the historic rate of earthquakes has been low by a factor of 2 or more compared to our model. Most historical moment release in this region occurred between 1857-1887, demonstrating the highly episodic character of large earthquakes in the region.

Conclusions

We have summed the overall seismic moment rates of all potential sources of large earthquakes in the NCEP model for the San Andreas fault system in northern California. We have compared this sum to essentially independent data: global tectonic models, VLBI observations, regional crustal strain observations, and the historical earthquake record (Table 4 and preceding discussion). We find the close agreement of all of these diverse data to be a reassuring quality check for the needs of regional seismic hazard mapping.

Although we believe the model is internally consistent and fully adequate for the present purpose given our present state of knowledge, many useful avenues of research remain to be explored to improve future hazard maps and other forms of hazard mitigation such as forecasting future events. Of particular note is a continuing need for the extension of the geodetic monitoring network into the more remote regions of high hazard that are still poorly known such as the northern Coast Range and the Modoc Plateau. The distribution of creeping and locked behavior is virtually unknown for several fault segments in the northern Coast Range, thus, monitoring the region could have important impact on understanding both the local hazards and the San Andreas fault system as a whole. Many more paleoseismological studies are required along the major strike-slip faults in the urban areas to improve forecasting of future events. Paleoseismic work is also

needed in the North Coast region to clarify system-wide issues of great seismic cycles and for a detailed understanding of each fault subsystem. Monitoring of microseismicity remains an essential tool both for delineating potential earthquake sources on poorly-mapped active faults and as a means of testing current ideas about the migration of stress changes in such complex tectonic regimes as the northern Coast Range.

Appendix A

The database: structure, limitations and accessibility

The database, simplified into Table A-1 and Figure 2 was created as a searchable GIS-database using MapInfo® software and can be downloaded by anonymous FTP as export files (ncep9606.mid and .mif). An ArcInfo® export file is also available (ncep9606.e00). The FTP site is currently on **andreas.wr.usgs.gov** in directory /pub/outgoing/lienkaemper/NCEP. Material related to the database, including many color figures, can be browsed or downloaded from the Internet at **http://eratos.wr.usgs.gov/NCEP/**. If these sites change, links may be found on the Northern California home page for the USGS earthquake program located at **http://quake.wr.usgs.gov**/. USGS does not warrant the suitability of this database or other materials available at these Internet sites for use in other applications. Representation of fault zones is highly simplified specifically for this application. The database is a USGS product and is not copyrighted, however some materials available by Internet related to the creation of this database may be subject to copyright laws, and as such, users are responsible for any further use they make of these materials.

Acknowledgments

References

Anderson, L. W., Anders, M.H., and Ostenaa, D.A., 1982, Late Quaternary faulting and seismic hazard potential eastern Diablo Range, California: California Division of Mines and Geology Special Publication, v. 62, p. 197-206.

Anderson, R. S., and Menking, K. M., 1994, The Quaternary marine terraces of Santa Cruz, California: evidence for coseismic uplift on two faults: Geological Society of America Bulletin, v. 106, no. 5, p. 649-664.

Andrews, D. J., Oppenheimer, D. H., and Lienkaemper, J. J., 1993, The Mission Link between the Hayward and Calaveras faults: Journal of Geophysical Research, v. 98, no. B7, p. 12,083-12,095.

Argus, D. F., and Gordon, R.G., 1991, Current Sierra Nevada- North American motion from very long baseline interferometry—implications for the kinematics of the western United States: Geology, v. 19, p. 1085-1088.

Bakun, W. H., King, G. C. P., and Cockerham, R. S., 1986, Seismic slip, aseismic slip, and the mechanics of repeating earthquakes on the Calaveras fault, California: Earthquake Source Mechanics, Geophysical Monograph 37, Am. Geophys. Union, p. 195-207.

Bonilla, M. G. and Lienkaemper, J. J., 1990, Visibility of fault strands in exploratory trenches and timing of rupture events: Geology, v. 18, no. 2, p. 153-156.

Bortugno, E. J., McJunkin, R.D., and Wagner, D.L., 1992, Map showing recency of faulting, San Francisco-San Jose quadrangle, California: California Division of Mines and Geology Regional Geologic Map Series, Map 5A, Sheet 5, map scale 1:250,000.

Bryant, W. A., Smith, D.P., and Hart, E.W., 1981, Sargent, San Andreas and Calaveras fault zone--evidence for recency in the Watsonville East, Chittenden and San Felipe quadrangles, California: California Division of Mines and Geology Open-File Report 81-7 SF (3 map sheets at 1:24,000 scale).

Bryant, W. A., 1985, Faults in the southern Monterey Bay area, Monterey County: California Division of Mines and Geology Fault Evaluation Report FER-167 [unpublished report, included in archive, staff, CDMG, 1990].

Castillo, D. A., and Ellsworth, W. L., 1993, Seismotectonics of the San Andreas fault system between Point Arena and Cape Mendocino in northern California: implications for the development and evolution of a young transform: Journal of Geophysical Research, v. 98, no. B4, p. 6543-6560.

CDMG staff, 1990, Microfiche copies of Fault Evaluation Reports for the southern Coast Ranges: California Division of Mines and Geology Open-File Report 90-11, 4 p., 1 pl. and microfiche archive.

Clark, M. M., Harms, K.K., Lienkaemper, J.J., Harwood, D.S., Lajoie, K.R., Matti, J.C., Perkins, J.A., Rymer, M.J., Sarna-Wojcicki, A.M., Sharp, R.V., Sims, J.D., Tinsley, J.C. III, and Ziony, J.I., 1984, Preliminary slip-rate table and map of late-Quaternary faults of California: U.S. Geological Survey Open-File Report 84-106; 12 p., 5 plates, map scale 1:1,000,000.

Cockerham, R. S., Lester, F. W., and Ellsworth, W. L., 1980, A preliminary report on the Livermore Valley earthquake sequence January 24-February 26, 1980: U.S. Geological Survey Open-File Report 80-714; 54 p.

Cooper, A., 1973, Structure of the continental shelf west of San Francisco, California: U.S. Geological Survey Open-File Report 73-1907; 65 p.

Coppersmith, K. J., 1979, Activity assessment of the Zayante-Vergeles fault, central San Andreas fault system, California: University of California, Santa Cruz, unpub. Ph.D. dissertation, 210 p.

DeMets, C., Gordon, R.G., Argus, D.F., and Stein, S., 1994, Effects of recent revisions to the geomagnetic reversal of time scale on estimates of current plate motions: Geophysical Research Letters, v. 21, no. 20, p. 2191-2194.

DeMets, C., 1995, A reappraisal of seafloor spreading lineations in the Gulf of California: Implications for the transfer of Baja California to the Pacific plate and estimates of Pacific-North America motion: Geophysical Research Letters, v. 22, no. 24, p. 3545-3548.

Dixon, T. H., Robaudo, S., Lee, J., and Reheis, M.C., 1995, Constraints on present-day Basin and Range deformation from space geodesy: Tectonics, v. 14, p. 755-772.

Ellsworth, W. L., Olson, J. A., Shijo, L. N. and Marks, S. M., 1982, Seismicity and active faults in the eastern San Francisco Bay region: California Division of Mines and Geology Special Publication, v. 62, p. 83-91.

Ellsworth, W. L., 1990, 6. Earthquake history , 1769-1989 in R. E. Wallace, ed., The San Andreas Fault System: U.S. Geological Survey Professional Paper 1515, p. 153-187.

Feigl, K. L., Agnew, D. C., Bock, Y., Dong, D., Donnellan, A., Hager, B. H., Herring, T. A., Jackson, D. D., Jordan, T. H., King, R. W., Larsen, S., Larson, K. M., Murray, M. H., Shen, Z., and Webb, F. H., 1993, Space geodetic measurement of crustal deformation in central and southern California, 1984-1992: Journal of Geophysical Research, v. 98, no. B12, p. 21,677-21,712.

Frankel, A., Mueller, C., Barnhard, T., Perkins, D., Leyendecker, E.V., Dickman, N. Hanson, S., and Hopper, M., 1996, National Seismic Hazard Maps: Documentation June 1996: U.S. Geological Survey Open-File Report 96-532, p. 44.

Galehouse, J. S., 1995, Theodolite measurements of creep rates on San Francisco Bay region faults: U.S. Geological Survey Open-File Report 95-210, p. 335-346.

Gordon, R. G., and D. F. Argus, 1993, The San Andreas fault system in central California as the boundary between the Pacific and the Sierra Nevada-Great Valley microplate: kinematics from VLBI geodesy (abs.): Eos (American Geophysical Union, Transactions), v. 74, p. 64.

Hall, N. T., Hunt, T. D., and Vaughan, P. R., 1994, Holocene behavior of the San Simeon fault zone, south-central coastal California: Geological Society of America Special Paper, v. 292, p. 167-189.

Hall, N. T., Wright, R. H., and Clahan, K. B., 1995, Final technical report, paleoseismic investigations of the San Andreas fault on the San Francisco Peninsula, California: USGS-NEHRP contract report, #14-08-0001-G2081, on file at U.S. Geological Survey, Reston, VA; 45 p., 26 figs., 2 tables, 27 plates.

Hanks, T. C., and Kanamori, H., 1979, A moment-magnitude scale: Journal of Geophysical Research, v. 84, p. 2348-2350.

Hanks, T. C., and Krawinkler, H., 1991, The 1989 Loma Prieta, California, earthquake and its effects: Introduction to the special issue: Seismological Society of America Bulletin, v. 81, p. 1415-1423.

Hanson, K. L., and Lettis, W. R., 1994, Estimated Pleistocene slip rate for the San Simeon fault zone, south-central coastal California: Geological Society of America Special Paper, v. 292, p. 133-150.

Harlan Tait Associates, 1994, Fault and limited geotechnical investigation North Fairfield site, Fairfield, California: public-access geotechnical report, City of Fairfield, 41 p. and illustrations.

Harms, K. K., Harden, J.W., and Clark, M.M., 1987, Use of quantified soil development to determine slip rates on the Paicines fault, northern California (abs.): Geological

Society of America Abstracts with Programs, 83rd Meeting, Cordilleran Section, v. 19, no. 6, p. 387.

Hart, E. W., Bryant, W.A., Manson, M.W., and Kahle, J.E., 1986, Summary report, Fault evaluation program, 1984-1985, southern Coast Ranges region and other areas: California Division of Mines and Geology Open-File Report 86-3, 26 p., 1 plate, scale 1:500,000.

Hedel, C. W., 1984, Maps showing geomorphic and geologic evidence for late Quaternary displacement along the Surprise Valley and associated faults, Modoc County, California: U.S. Geological Survey Miscellaneous Field Studies Map MF-1429, 2 sheets, scale 1:62,500.

Hitchcock, C. S., Kelson, K. I., and Thompson, S. C., 1994, Geomorphic investigations of deformation along the northeastern margin of the Santa Cruz Mountains: U.S. Geological Survey Open-File Report 94-187; 51 p., 2 pl.

Jennings, C. W., 1977, Geologic Map of California, 1:750,000: California Division of Mines and Geology, Geologic Data Map No.2.

Jennings, C. W., 1992, Preliminary fault activity map of California: California Division of Mines and Geology Open-File Report 92-3, scale 1:750,000.

Jennings, C. W., 1994, Fault activity map of California and adjacent areas with locations and ages of recent volcanic eruptions: California Division of Mines and Geology Data Map Series No. 6, 92 p., 2 plates, map scale 1:750,000.

Kelson, K. I., Simpson, G. D., Lettis, W. R., and Haraden, C. C., 1996, Holocene slip rate and recurrence of the northern Calaveras fault at Leyden Creek, eastern San Francisco Bay region: Journal of Geophysical Research, v. 101, no. B3, p. 5961-5975.

Knuepfer, P. L., 1977, Geomorphic investigations of the Vaca and Antioch fault systems, Solano and Contra Costa Counties, California: Stanford University, Stanford, California, M.S. thesis, 53 p.

LaForge, R., and Lee, W. H. K., 1982, Seismicity and tectonics of the Ortigalita fault and southeast Diablo Range, California: California Division of Mines and Geology Special Publication, v. 62, p. 93-101.

Lawson, A. C., 1908, The earthquake of 1868 in A. C. Lawson, ed., The California earthquake of April 18, 1906: Report of the State Earthquake Investigation Commission (Volume I): Carnegie Institution of Washington Publication No. 87, p. 434-448.

Lettis, W. R., 1982, Late Cenozoic stratigraphy and structure, central San Joaquin Valley, California: U.S. Geological Survey Open-File Report 82-526, 203 p., scale 1:500,000.

Lienkaemper, J. J., G. Borchardt, and M. Lisowski, 1991, Historic creep rate and potential for seismic slip along the Hayward fault, California: Journal of Geophysical Research, v. 96, no. B11, p. 18,261-18,283.

Lienkaemper, J. J., 1992, Map of recently active traces of the Hayward fault, Alameda and Contra Costa Counties, California: U.S. Geological Survey Miscellaneous Field Studies Map MF-2196, map scale 1:24,000, p. 13.

Lienkaemper, J. J., and Prescott, W. H., 1989, Historic surface slip along the San Andreas fault near Parkfield, California: Journal of Geophysical Research, v. 94, no. B12, p. 17,647-17,670.

Lienkaemper, J. J., Williams, P. L., Taylor, P., and Williams, K., New evidence of large surface-rupturing earthquakes along the northern Hayward fault zone [abstr.]: SEPM (Society of Economic Paleontologists and Mineralogists) Pacific Section, 70th Annual Meeting, San Francisco, California, 1995, SEPM, p. 38.

Lienkaemper, J. J., and Borchardt, G., 1996, Holocene slip rate of the Hayward fault at Union City, California: Journal of Geophysical Research, v. 101, no. B3, p. 6099-6108.

Lisowski, M., and Prescott, W. H., 1989, Strain accumulation near the Mendocino triple junction [abstr.]: Eos (American Geophysical Union, Transactions), v. 70, no. 43, p. 1332.

Lisowski, M., Prescott, W. H., Savage, J. C., and Johnston, M. J., 1990, Geodetic estimate of coseismic slip during the 1989 Loma Prieta, California, earthquake: Geophysical Research Letters, v. 17, no. 9, p. 1437-1440.

Louderback, G. D., 1947, Central California earthquakes of the 1830's: Seismological Society of America Bulletin, v. 34, no. 1, p. 33-74.

Machette, M. N., Personius, S.F., and Nelson, A.R., 1992, Paleoseismology of the Wasatch fault zone: U.S. Geological Survey Professional Paper, v. 1500-A, p. 72 p.

McCarthy, J., Hart, P. E., and Oppenheimer, D., High-angle faulting in the western Sacramento delta region, Pittsburg, California: SEPM (Society of Economic Paleontologists and Mineralogists) Pacific Section, 70th Annual Meeting, San Francisco, California, 1995, SEPM, p. 39.

McCrory, P. A., 1996, Evaluation of fault hazards, northern coastal California: U.S. Geological Survey Open-File Report 96-657, 87 p.

McCulloch, D. S., 1987, Regional geology and hydrocarbon potential of offshore central California in G. D. W. Scholl A., and Vedder, J. G., ed., Geology and resource potential of the continental margin of western North America and adjacent ocean basins——Beaufort Sea to Baja California: Circum Pacific Council for Energy and Mineral Resources, Earth Science Series 6, p. 353-401.

McCulloch, D. S., and Greene, H.G., 1990, Geologic map of the central California continental margin, Map No. 5A (Geology) in H. G. Greene and Kennedy, M.P., ed., California Division of Mines and Geology California Continental Margin Geologic Map Series, Area 5 of 7, map scale 1:250,000:.

Murray, M. H., Marshall, G.A., Lisowski, M. and Stein, R.S., 1996, The 1992 M=7 Cape Mendocino, California earthquake: coseismic deformation at the south end of the Cascadian megathrust: Journal of Geophysical Research, v. 101, no. B8, p. 17,707-17,726.

Niemi, T. M., and Hall, N. T., 1992, Late Holocene slip rate and recurrence of great earthquakes on the San Andreas fault in northern California: Geology, v. 20, no. 3, p. 196-198.

Nolan, J. M., Zinn, E.N., and Weber, G.E., 1995, Paleoseismic study of the southern Sargent fault, Santa Clara and San Benito Counties California: U.S. Geological Survey NEHRP Final Technical Report 1434-94-G-2466, 23 p. [contract report on file at U.S. Geological Survey, Menlo Park, California].

Oppenheimer, D. H., Bakun, W. H., and Lindh, A. G., 1990, Slip partitioning of the Calaveras fault, California, and prospects for future earthquakes: Journal of Geophysical Research, v. 95, no. B6, p. 8483-8498.

Oppenheimer, D. H., and Lindh, A. G., 1993, The potential for earthquake rupture of the northern Calaveras fault: California Division of Mines and Geology Special Publication, v. 113, p. 233-240.

Oppenheimer, D. H., Wong, I. G., and Klein, F. W., 1993, The seismicity of the Hayward fault, California: California Division of Mines and Geology Special Publication, v. 113, p. 91-100.

Page, W. D., and Renne, P. R., 1994, 40AR-39AR dating of Quaternary basalt, western Modoc Plateau, northeastern California: Implications to tectonics [abstr.]: U.S. Geological Survey Circular 1107 [Abstracts of the Eighth International Conference on Geochronology, Cosmochronology and Isotope Geology, Lanphere, M. A., Dalrymple, G. B., and Turrin, B. D. (eds.)], p. 240.

Perkins, J. A., and Sims, J.D., 1988, Late Quaternary slip along Calaveras fault near Hollister, California: Eos (American Geophysical Union, Transactions), v. 69, no. 44, p. 1420.

Petersen, M. D., Bryant, W.A., Cramer, C.H., Cao, T., Reichle, M.S., Frankel, A.D., Lienkaemper, J.J., McCrory, P.A., and Schwartz, D.P., 1996a, Seismic hazard assessment for the State of California: Eos (American Geophysical Union, Transactions), v. 77, no. 44, p. F506.

Petersen, M. D., Bryant, W.A., Cramer, C.H., Cao, T., Reichle, M.S., Frankel, A.D., Lienkaemper, J.J., McCrory, P.A., and Schwartz, D.P., 1996b, Probabilistic seismic hazard assessment for the State of California: California Division of Mines and Geology Open-File Report issued jointly with U.S. Geological Survey, CDMG 96-___ and USGS 96-706, ~52 p.,

Pezzopane, S. K., 1993, Active faults and earthquake ground motions in Oregon: University of Oregon, Ph. D. dissertation, 208 p.

Phipps, S. P., 1992, Late Cenozoic tectonic wedging and blind thrusting beneath the Sacramento Valley and eastern Coast Ranges, Day 2: American Association of Petroleum Geologists. Pacific Section. Guidebook, v. 70, p. 63-84.

Prentice, C. S., 1989, Earthquake geology of the northern San Andreas fault near Point Arena California: California Institute of Technology, Pasadena, unpub. Ph.D. dissertation, 252 p.

Prentice, C., Niemi, T. N., and Hall, N. T., 1991, Quaternary tectonics of the northern San Andreas fault, San Francisco Peninsula, Point Reyes, and Point Arena, California [field trip guide]: California Division of Mines and Geology Special Publication, v. 109, p. 25-34.

Prescott, W. H., and Burford, R. O., 1976, Slip on the Sargent fault: Seismological Society of America Bulletin, v. 66, no. 3, p. 1013-1016.

Prescott, W. H., and M. Lisowski, 1983, Strain accumulation along the San Andreas fault system east of San Francisco Bay, California: Tectonophysics, v. 97, p. 41-56.

Prescott, W. H., King, N. E., and Gu, G. H., 1984, Preseismic, coseismic and postseismic deformation associated with the 1984 Morgan Hill, California, earthquake: California Division of Mines and Geology Special Publication, v. 68, p. 137-148.

Rogers, J. D., and Halliday, J. M., 1993, Exploring the Calaveras-Las Trampas fault junction in the Danville-San Ramon area: California Division of Mines and Geology Special Publication, v. 113, p. 261-270.

Savage, J. C., Prescott, W.H., Lisowski, M., and King, N., 1979, Geodolite measurements of deformation near Hollister, California, 1971-1978: Journal of Geophysical Research, v. 84, p. 7599-7615.

Savage, J. C., Lisowski, M., and Prescott, W.H., 1992, Strain accumulation across the Wasatch fault near Ogden, Utah: Journal of Geophysical Research, v. 97, no. B2, p. 2071-2083.

Savage, J. C., and Lisowski, M., 1993, Inferred depth of creep on the Hayward fault, central California: Journal of Geophysical Research, v. 98, no. B1, p. 787-793.

Savage, J. C., Lisowski, M., Svarc, J.L., and Gross, W.K., 1995, Strain accumulation across the Central Nevada Seismic Zone, 1973-1994: Journal of Geophysical Research, v. 100, no. B10, p. 20,257-20,269.

Schwartz, D. P., and Coppersmith, K. J., 1984, Fault behavior and characteristic earthquake--examples from the Wasatch and San Andreas fault zones: Journal of Geophysical Research, v. 89, no. B7, p. 5681-5698.

Schwartz, D. P., Pantosti, D., Hecker, S., Okamura, K., Budding, K. E., and Powers, T., 1993, Late Holocene behavior and seismogenic potential of the Rodgers Creek fault zone, Sonoma County, California: California Division of Mines and Geology Special Publication, v. 113, p. 393-398.

Schwartz, D. P., Joyner,W.B., Stein, R.S., Brown, R.D., McGarr, A.F., Hickman, S.H., and Bakun, W.H., 1996, Review of seismic-hazard issues associated with the Auburn Dam project, Sierra Nevada foothills, California: U.S. Geological Survey Open-File Report 96-11, 8 p.

Schwartz, D. P., Pantosti, D., Okumura, K., Powers, T., and Hamilton, J., 1997, Recurrence of large magnitude earthquakes in the Santa Cruz Mountains, California— Implications for behavior of the San Andreas Fault: Journal of Geophysical Research (in review, to be submitted).

Sieh, K. E., and Jahns, R.H., 1984, Holocene activity of the San Andreas fault at Wallace Creek, California: Geological Society of America Bulletin, v. 95, p. 883-896.

Simpson, G. D., and Lettis, W.R., 1994, Paleoseismic investigation of the northern Calaveras fault: U.S. Geological Survey Open-File Report 94-176, p. 660-661.

Simpson, G. D., Lettis, W. R., and Kelson, K. I., 1993, Segmentation model for the northern Calaveras fault, Calaveras Reservoir to Walnut Creek: California Division of Mines and Geology Special Publication, v. 113, p. 253-259.

Sims, J. D., 1991, Distribution and rate of slip across the San Andreas transform boundary, Hollister area, central California: Geological Society of America Abstracts with Programs, 87th Meeting Cordilleran Section, v. 23, no. 2, p. 98.

Snyder, D. L., Wills, C. J., and Borchardt, G., 1995, Slip rate and earthquake recurrence on the Concord fault at Galindo Creek, Concord, California: USGS-NEHRP contract report, #1434-94-G2483 [contract report on file at U.S. Geological Survey, Reston, VA, 37 p.].

Sowers, J. M., Noller, J. S., and Unruh, J. R., 1993, Quaternary deformation and blind-thrust faulting on the east flank of the Diablo range near Tracy, California: California Division of Mines and Geology Special Publication, v. 113, p. 377-383.

Stein, R. S., and Ekström, G., 1992, Seismicity and geometry of a 110-km-long blind thrust fault: 2. Synthesis of the 1982-1985 [Coalinga] California earthquake sequence: Journal of Geophysical Research, v. 97, no. B4, p. 4865-4883.

Thatcher, W., Marshall, G., Lisowski, M., 1997, Resolution of fault slip along the 470-km-long rupture of the great 1906 San Francisco earthquake: Journal of Geophysical Research [preprint, in review], v. 102.

Toppozada, T. R., Borchardt, G., Hallstrom, C. L., and Youngs, L. G., 1993, Planning scenario for a major earthquake on the Hayward fault: California Division of Mines and Geology Special Publication, v. 113, p. 457-462.

Toppozada, T. R., and Borchardt, G., 1996, Relocation of the 1836 "Hayward fault" earthquake to near San Juan Bautista and reevaluation of the 1838 San Andreas earthquake: Seismological Society of America Bulletin (to be submitted).

Tuttle, M., and Sykes, L., 1993, Re-evaluation of the 1838, 1865, 1868, and 1890 earthquakes in the San Francisco Bay area: California Division of Mines and Geology Special Publication, v. 113, p. 81-89.

Unruh, J. R., and Moores, E. M., 1992, Quaternary blind thrusting in the southwestern Sacramento Valley, California: Tectonics, v. 11, no. 2, p. 192-203.

Unruh, J. R., Loewen, B. A., and Moores, E. M., 1995a, Progressive arcward contraction of a Mesozoic-Tertiary fore-arc basin, southwestern Sacramento Valley, California: Geological Society of America Bulletin, v. 107, no. 1, p. 38-53.

Unruh, J. R., Simpson, G. D., Hitchcock, C. S., and Lettis, W. R. [of W. R. Lettis and Associates], 1995b, Seismotectonic evaluation, Stony Gorge and East Park Dams, Orland Project, northern Coast Ranges, California: Draft report prepared for U.S. Bureau of Reclamation, 170 p.

Wakabayashi, J., and Smith, D. L., 1994, Evaluation of recurrence intervals, characteristic earthquakes, and slip rates associated with thrusting along the Coast Range-Central Valley geomorphic boundary, California: Seismological Society of America Bulletin, v. 84, no. 6, p. 1960-1970.

Wald, D. J., Heaton, S. H., and Helmberger, D. V., 1991, Rupture model of the 1989 Loma Prieta earthquake from the inversion of strong motion and broadband teleseismic data: Seismological Society of America Bulletin, v. 91, p. 1540-1572.

Wald, D. J., Kanamori, H., Helmberger, D. V., and Heaton, T. H., 1993, Source study of the 1906 San Francisco earthquake: Seismological Society of America Bulletin, v. 83, no. 4, p. 981-1019.

Ward, S. N., 1990, Pacific-North America Plate Motions—New results from Very Long Baseline Interferometry: Journal of Geophysical Research, v. 95, no. B13, p. 21,965-21,981.

Weber, G. E., 1981, Geologic investigation of the marine terraces of the San Simeon region and Pleistocene activity on the San Simeon fault zone, San Luis Obispo County, California: USGS-NEHRP contract report, #14-08-0001-18230, on file at U.S. Geological Survey, Reston, VA; 66 p.

Weber, G. E., and Nolan, J. M., 1995, Determination of late Pleistocene-Holocene slip rates along the San Gregorio fault zone, San Mateo County, California: U.S. Geological Survey Open-File Report 95-210, p. 805-807.

Wells, R. E., 1990, Paleomagnetic rotations and the Cenozoic tectonics of the Cascade Arc, Washington, Oregon, and California: Journal of Geophysical Research, v. 95, no. B12, p. 19,409-19,417.

Wells, D. L., and Coppersmith, K. J., 1994, New empirical relationships among magnitude, rupture length, rupture width, rupture area, and surface displacement: Seismological Society of America Bulletin, v. 84, no. 4, p. 974-1002.

Williams, P. L., 1993, Geologic record of southern Hayward fault earthquakes: California Division of Mines and Geology Special Publication, v. 113, p. 171-179.

Williams, P. L., Anima, R. , Ingram, L. , McCarthy, J., McEvilly, T. V., Nakata, T. , Okamura, M., and Shimazaki, K., 1997, Geometry and Holocene activity of the Pinole and southernmost Rodgers Creek faults, San Pablo Bay, California: Geological Society of America Bulletin [preprint, in review].

Wills, C. J., and Borchardt, G., 1993, Holocene slip rate and earthquake recurrence on the Honey Lake fault zone, northeastern California: Geology, v. 21, no. 9, p. 853-856.

Wong, I. G., and Hemphill-Haley, M.A., 1993, Seismicity and faulting near the Hayward and Mission faults: California Division of Mines and Geology Special Publication, v. 113, p. 207-215.

Working Group on California Earthquake Probabilities, 1988, Probabilities of large earthquakes occurring in California on the San Andreas fault: U.S. Geological Survey Open-File Report 88-398, 62 p.

Working Group on California Earthquake Probabilities, 1990, Probabilities of large earthquakes in the San Francisco Bay Region, California: U.S. Geological Survey Circular, v. 1053, p. 51.

Wright, R. H., Hamilton, D. H., Hunt, T. D., Traubenik, M. L., and Shlemon, R. J., 1982, Character and activity of the Greenville structural trend: California Division of Mines and Geology Special Publication, v. 62, p. 187-196.

Yu, E., and Segall, P., 1996, Slip in the 1868 Hayward earthquake from the analysis of historical triangulation data: Journal of Geophysical Research, v. 101, no. B7, p. 16,101-16,118.

Figure Captions

Figure 1. Comparison of historically observed moment magnitudes in northern California with the empirical rupture area and length relations of *Wells and Coppersmith* [1994]

Figure 2. Location map showing segmentation of faults labeled by codes (*e.g.,* **H2**) that appear in Table A-1. Segment ends shown as X ; Great Valley blind thrusts as dashed lines with ticks; areal sources by dashed polygons labeled near centers. Faults with slip rate >1 mm/yr shown with thickness proportionate to slip rate. Locations: GG, Golden Gate; HOL, Hollister; MTJ, Mendocino triple junction; SJB, San Juan Bautista.

Figure 3. 1906 slip from analysis of triangulation by *Thatcher and others* [1997]. Lithic patterns indicate extent of hypothetical segments (**A2** and **A3**) where independent rupture is assumed.

Figure 4. Cartoon shows hypothetical sequence of slip accumulation along the joint San Andreas, San Gregorio and Sargent fault system.

Figure 5. Segmentation of Calaveras and Hayward faults. Circles show M≥2 recent seismicity 1989-95; stars, historic events M≥5.7 [*Ellsworth,* 1990] by year and magnitude. Open squares, trench sites (CA, Camille Ave.; LC, Leyden Creek; MH, Masonic Home; MT, Montclair; TP, Tule Pond; WC, Welch Creek); closed squares, trilateration arrays (VA, Veras; HV, Grant Ranch in Halls Valley); triangle SF19, alinement array. Locations: AC; Agua Caliente Creek; BT, BART tunnel; CR, Calaveras Reservoir; DC, Dublin Canyon; ER, Ellworthy Ranch; MC, Mills College; SL, San Leandro

Figure 6. Hayward fault, historic earthquakes. Cartoon showing assumed locking patches at depth. See text for further discussion and explanation. Abbreviations as in Figure 5.

Figure 7. Hypothetical slip accumulation along Northern Calaveras fault. See text for further discussion.

Figure 8. North Coast seismicity (upper map, USGS catalog, 1968-1985) and creep localities (lower map). Rectangular area near Geysers (near **L08**) has seismicity deleted. Creep localities and geodetic sites marked by large triangles for alinement arrays and by small triangles with vectors for USGS trilateration stations and velocity analysis of M. H. Murray (unpub. data, 1996). Velocity vectors (arrows) indicate net right-lateral from P (Poonkinney) to Covelo of 8.3 mm/yr (1985-1989). See Figure 2a for location map of segments: **C5**, **C6**, **C7**, **C8**, **H4**, **H5**, **H6** and **H7**

Figure 9. Great Valley thrust faults. Segments used in this study (**GV01**-**GV14**); heavy dashed lines indicate blind thrust tips buried at 7 km depth. Gray rectangles show downdip extent of these hypothetical ruptures. Segments of *Wakabayashi and Smith* [1994](labeled **WS-1** to **WS-17**) based mainly on geomorphic interpretation of range front. Quaternary faults of *Jennings* [1992] shown as dark lines for youngest faults and narrower gray lines for oldest faults. Other lines: antiforms (dashes and pluses), major piercements (MDA, Mount Diablo; NIA, New Idria) and surficial thrusts (continuous ticks, on hanging wall) [*Jennings,* 1977; *Phipps,* 1992]. Along Sacramento Valley margin, fine black lines indicate interpreted subsurface ramps (arrow lines point up-dip), flats (T's) and subsurface thrust tips (2-tick dashes) of *Unruh and others* [1995b]. Historical earthquakes shown as stars attributed by magnitude and year of occurrence [*Ellsworth,* 1990.]

Figure 10. Path across northern Great Basin and San Francisco Bay area for summation of long-term geologic slip vectors on active fault systems. Faults: SA, San Andreas; H, Hayward; C, Calaveras; GV, Great Valley thrusts; HL, Honey Lake; L, Likely; SV, Surprise Valley; BR, Black Rock; JM, Jackson Mountains. L-T TZ, Lassen-Tahoe tectonic zone. Stars, Holocene volcanic centers (MLV, Medicine Lake volcano). Triangles, VLBI sites (HTC, Hat Creek)

Figure 11. Slip vectors assumed for this study shown as solid arrows and solid lines.

Figure 12. San Andreas fault system. Historical earthquakes [stars annotated by year and magnitude; *Ellsworth,* 1990; 1836 earthquake, *Toppozada and Borchardt*, 1997]. Simplified plate boundary, short-dashed line. Perimeter for summing of earthquake moment for Figure 13 shown by long-dashed line. GG, Golden Gate; MTJ, Mendocino triple junction; PKF, Parkfield

Figure 13. Moment Rate of Model vs Historical Earthquakes. Only 50-70% of main seismic cycle has occurred in the historical period.